Investigation of Electrospun Nanofibrous Scaffold Mechanical Properties

S. Farboodmanesh, J. Chen, J. L. Pelealuw, and D. E. Cloutier
Advanced Composite Materials and Textile Research Lab. (ACMTRL), Mechanical Engineering Dept.,
University of Massachusetts Lowell,
One University Avenue, Lowell, MA 01854

1 ABSTRACT

There has been considerable growth and development in electrospun nanofibers for research activities, as well as commercial fabrication over the past decade. These continuous nanofibers are fabricated from solution, driven primarily by an electric field. One key application of interest is the creation of tissue scaffolds via electrospinning. Although numerous studies have been conducted on electrospun fibrous scaffolds, there is still an Edisonian-type process to acquire the desired scaffold orientation and mechanical response that mimics the native tissue behavior. In this study, the electrospun scaffolds are fabricated with different fiber orientation – e.g. aligned and random – over large areas and lengths. The mechanical behavior of the electrospun scaffolds and of the individual fibers (using AFM probe) are investigated. The results obtained from both methods were compared to determine if composite mechanics models can be applied to predict and design the desired fiber orientations to provide sufficient mechanical behavior and cell support for a native tissue.

Keywords: electrospun fibers (aligned and random), nanofibrous scaffolds, scaffolds mechanical behavior

2 INTRODUCTION

Nanofibers can be produced from several processes – e.g., self-assembly, nanolithography, bicomponent sea-island melt extrusion, and electrospinning. Most of these methods represent trade-offs between high-accuracy and high-volume [1]. Electrospinning is the method that was chosen for this study of nanofibrous scaffold, since by manipulating the setup and process parameters, one can replicate and mimic the extracellular matrices (ECM) of native tissues. The electrospinning process can also be modified so that the average fiber diameter can range from a few micrometers to tens of nanometers.

Electrospinning starts with a pendant droplet (Taylor cone) formed at the tip of a pipette/syringe. Upon applying a high voltage to the polymer solution or melt, the charged droplet elongates towards the target and forms a jet when the applied electric field exceeds the surface tension forces. Initially the jet path is straight from the pipette tip, but then instability causes a bending or whipping motion, resulting in a conical path about the same axis. This elongated path is responsible for the high draw ratio that reduces the jet diameter significantly relative to the pipette tip diameter. Moreover, the solvent continues to evaporate, increasing the solids content and further reducing the fiber diameter. Eventually a nonwoven semi-dry fiber mat is formed on the target [2]. For a variety of polymer-solvent combinations, the important process parameters are the solution properties, electric field strength, feed rate, and environmental conditions – e.g., humidity.

Numerous studies have demonstrated that electrospun fibrous scaffolds can exhibit similar features to a native tissue structure, i.e., a hierarchical, fibrous, structural organization. A wide range of natural and biodegradable polymers have been electrospun into fibers for various *in vitro* cell interaction studies for blood vessel, heart valves, skin, bone, cartilage, and tendons [3–7]. The effect of nanoscale properties on cell growth and tissue response is unknown. Therefore, it is important to investigate the effect of different scaffold parameters – i.e., fiber orientation, fiber diameter, porosity, and mechanical behavior of fibrous mat/individual fiber – to enable development of composite hybrid structures to accomplish the desired functionality of replacement tissue. In addition, He, et al. [8] has shown that anisotropic fibrous tissue demonstrates a nonlinear mechanical behavior; therefore modeling such complex behavior is a formidable task. Thus, in this study, the effect of fiber orientation on mechanical properties – i.e., the relationship between individual nanofiber properties and the properties of random and oriented nanofibrous mats – is described. This will ultimately lead to an effective replication of the required composite stiffness for the desired complex mechanical behavior under normal physiological conditions as a native tissue.

3 MATERIALS AND EXPERIMENTAL SET-UP

3.1 Electrospinning of Controlled Orientation Fibers and Fiber Mats

The solution used for the electrospun fibers is an 8 wt% polyethylene oxide (PEO) with molecular weight of 200K, in ethanol and water (4:1) solution. PEO is chosen, due to ease of electrospinning with this material. Once the process is developed to create the continuous fibers and patterned structures, it is expected to be applicable to a wide range of polymers.

A flat aluminum (Al) and rotating target (Al strip with 2 cm width) is selected for different fiber orientation – i.e., aligned and random. The electric field for the experiments is 10 kV/m (regardless of the target geometry) and the

linear velocity for the rotating target is 15 m/s [9]. Figure 1 shows the schematic of the electrospinning setup for aligned orientation. Figures 2 and 3 illustrate field emission electron microscopy (FE-SEM) images of the resulting electrospun PEO nanofibers at 1000X magnification with the scale bar representing 10 μm. The fiber diameter for these specimens ranges from 500 nm to 1μm.

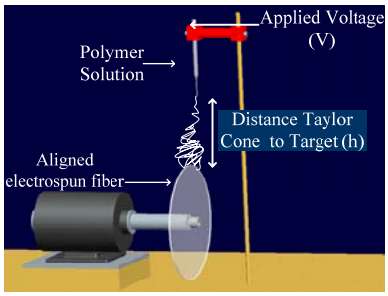

Figure 1 – Schematic of electrospinning set-up for aligned fibers

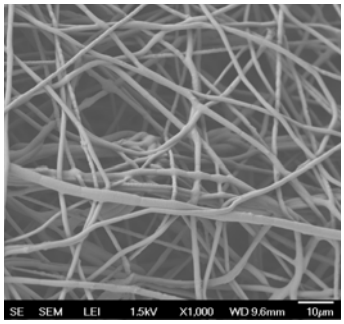

Figure 2 – FE-SEM of typical random electrospun PEO fiber mat (scale bar = 10 μm)

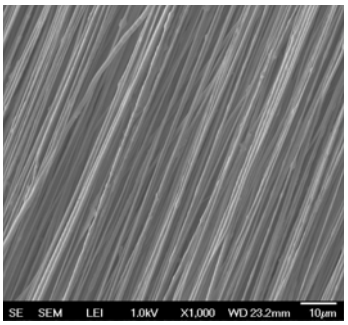

Figure 3 – FE-SEM of typical aligned (0^o) electrospun PEO fiber mat (scale bar = 10 μm).

To obtain individual electrospun nanofibers, several pieces of etched Si wafer (1 cm x 1cm) were placed on the rotating target disc edge with spinning time of 4 to 6 seconds. The Si is etched to create channels of different widths. Figure 4 presents several individual electrospun PEO fibers on a Si wafer at 500X.

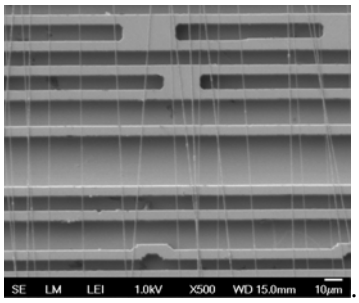

Figure 4 – FE-SEM of aligned electrospun PEO fibers on etched Si wafer (scale bar = 10 μm)

3.2 Mechanical Testing of Fiber Mats

Specimens of 25 mm x 12.5 mm (length x width) were cut from both random and aligned electrospun mats, and each specimen was framed. By framing the specimens the fiber deformation and applied preload during handling is minimized. The specimens are tested on an electromechanical Instron 4464 with a load cell of 1800 N (400 lb) and pneumatic grips. A 22.2 N (5 lb) load cell, LCFA-5 (OMEGA Engineering Inc., Stamford, CT), was mounted in series with the 4464 Instron load cell to obtain better resolution. The load is directly acquired from the small load cell, and the displacement is measured using a linear variable displacement transducer (LVDT) placed in contact with the Instron cross-head. The cross-head rate used for the tensile tests is 2.5 mm/min (0.1 in/min). Framed electrospun specimens are mounted in the pneumatic grips, and before starting the test the sides of the frame are cut, Figure 5(a).

Note that to obtain the effective thickness of the mat, specimens from the same electrospun batch and same dimensions were weighed using an Ohaus Adventurer Scale (AR3130, Pine Brook, NJ). Thus, by knowing the PEO density range (ρ=1.13–1.21 g/cm^3), the effective thickness of the specimens are determined, from assuming no air.

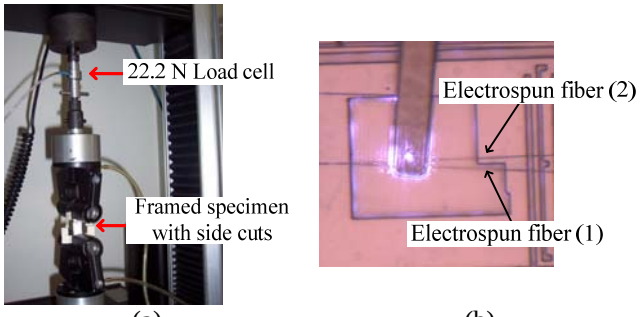

(a) (b)

Figure 5 – Mechanical testing setup for electrospun PEO, mat and individual fiber, (a) framed sample on Instron 4464 and 22 N load cell in series with the Instron load cell and (b) aligned fibers on etched Si wafer along with AFM probe.

3.3 Mechanical Testing of Individual Fibers

A PSIA (Fremont, CA) XE-100 atomic force microscope (AFM) was used for individual electrospun PEO fiber testing in contact mode. A 6-beam cantilever NSC12/tipless/AlBS (NSC: non-contact Si chip) with a spring constant of 0.3 N/m (MikroMasch USA, Wilsonville, OR) was used for this study. A 3-point bend test approach is used for this series of tests (alternative methods are currently being investigated), where the AFM probe is aligned at the center of a fiber suspended across a channel on the Si wafer and contacts the fiber in a downward motion at 0.5 μm/s. [10,11]. Load and displacement data is obtained from the AFM. Note that a tipless AFM probe was chosen to prevent any indentation or penetration through the fiber. Figure 5(b) shows the tipless AFM probe (top-view) with a width of 35 μm and two suspended electrospun fibers (each fiber diameter ~1 μm) with span lengths of 140 and 175 μm, respectively. To assure the anchoring of the fibers on the span edges, a few fibers were laterally displaced several microns (5-8 μm) by the AFM probe and no slippage was observed.

4 RESULTS AND DISCUSSIONS

4.1 Tensile Response of Electrospun Mat

Figure 6 shows the tensile behavior, average of 5 specimens, of both aligned and randomly-oriented electrospun mat with one standard deviation. Raw data from the test (load-displacement) was translated to stress (MPa)-strain (%).

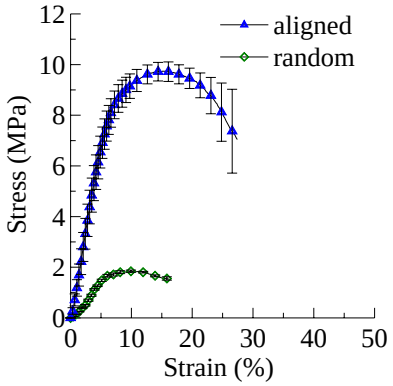

Figure 6 – Tensile behavior of aligned and random electrospun PEO fiber mats.

As expected, the aligned specimens exhibited higher tensile strength and stiffness compared to the random–orientation specimens. For the aligned specimen, all of the fibers are clamped on both ends; therefore, there is little to no fiber rotation within the samples, and the fibers are loaded in their direction of maximum stiffness and strength. In contrast, fibers in the random mat that are oriented off-axis (e.g., at 45°) to the loading direction contribute much less resistance to elongation. Therefore, the aligned mat shows higher elastic modulus (6X higher) and less strain compared to the random mat. Table 1 presents the averaged elastic moduli obtained for the electrospun mats.

Table 1 – Elastic modulus for electrospun fibers with aligned and random orientation

Fiber orientation	Elastic Modulus (MPa)
Aligned	122.5
Random	34

For a two-dimensional (2D) fibrous structure with random orientation the elastic modulus is presented in Equation 1 [12].

$$E_{2D} = \frac{3}{8}E_{11} + \frac{5}{8}E_{22} \quad (1)$$

where, E_{2D} is the elastic modulus of 2D rigid composite, E_{11} is the longitudinal elastic modulus of an aligned fiber layer and E_{22} is the transverse elastic modulus. Since $E_{11} >> E_{22}$ (Figure 7) and for the effective stiffness, E_{11}, only fiber was considered (no matrix) the $E_{2D} \approx \frac{3}{8}E_{11}$. From the modulus for electrospun random mat using E_f from aligned mat is 45 MPa. This value is about 30% higher than the obtained value from the experimental results, which might be the effect of fiber orientation.

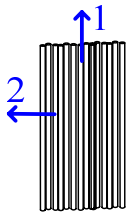

Figure 7 – Longitudinal and transverse directions (1 and 2, respectively) for fibrous composite structure.

4.2 Mechanical Response of Single Electrospun Fiber

Figure 8 shows a typical force-displacement curve measured by the AFM probe, where the AFM probe travels for about 3 μm downwards until it contacts the fiber. As the fiber is deflecting, the force increases to about 6 nN, and after a couple of microns of travel (as specified in the AFM program by the user), the probe returns to its original position.

NSTI-Nanotech 2008, www.nsti.org, ISBN 978-1-4200-8504-4 Vol. 2

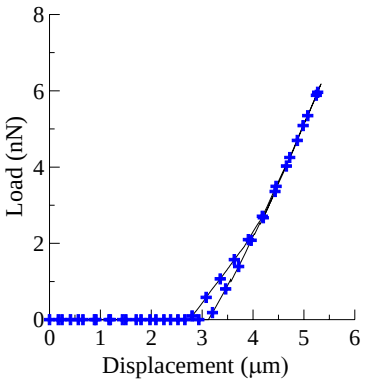

Figure 8 – Typical 3-point-bend test result for individual electrospun PEO fibers

As shown in Figure 5(b), there were actually two fibers in contact with the AFM probe. The fibers were suspended at two different spans – i.e., 140 and 175 μm. The raw data from the test (slope of load-displacement curve) was used for the standard equation for a clamped suspended beam with a circular cross-section (Equation 2). Because the two fibers were at different span lengths, equilibrium (measured load is the sum of the load on each fiber) and compatibility (both fibers have the same center displacement) can be used to obtain the correct elastic modulus for the fibers. In this case, the modulus (E) from the standard beam equation is multiplied by 0.3 if the longer span length is used, since the fiber 2 span is 80% of fiber 1, assuming both fibers have the same diameter (1 μm), see Figure 5(b).

$$E = \left(P/\delta\right)\left(KL_1^{\,3}/I\right) \qquad (2)$$

where P is the applied force (N) by AFM probe, δ is fiber displacement (m), L_1 is the span for fiber 1 (m), $I = \pi d^4/64$ where d represents the fiber diameter (m), and K=0.3 (when $L_2=0.8L_1$).

The resulting elastic modulus for the individual electrospun fiber PEO by AFM probe is 512 MPa.

4.3 Comparison of Single Fiber and Fiber Mat Moduli

There is about 5X difference in results obtained from the single fiber test (512 MPa) versus the E_f from the aligned scaffolds (122.5 MPa). This overestimate by the individual fiber testing is the effect of few assumptions made through the calculations. For example, the cantilever beam (AFM probe) actually applies a distributed load versus a point load, which is about 20% of the span. Taking this into account would reduce the calculated E_f. Note that also the two fibers diameter was assumed the same. If there is a variation in fiber diameter, for example fiber 1 diameter is about 60% of fiber 2 then the elastic modulus will be increased almost 3X, which will make the difference in results much larger. The effect of AFM probe width and modifications to thickness measurements are under investigation.

5 CONCLUSIONS

Mechanical response of electrospun PEO mat with different orientations, along with individual electrospun fibers were presented. The modulus of elasticity for random mat was reported 34 MPa versus the aligned mat which was 122.5 MPa. All of the fibers in aligned specimens are clamped which result in higher elastic modulus compared to random mat with their significant fiber rotation caused by off-axis fibers during the test. Individual electrospun fibers were tested by AFM probe in 3-point-bend test set-up. The elastic modulus from the AFM test presented a 5X increase compared to elastic modulus of fiber determined from aligned electrospun mat. These differences within the elastic moduli are effect of the assumptions for the calculations – e.g., cantilever geometry.

6 ACKNOWLEDGEMENTS

This work is supported by the Massachusetts Technology Collaborative (MTC), as part of the University of Massachusetts Lowell, Nanomanufacturing Center of Excellence (NCOE). The authors would like to acknowledge the assistance of Campus Materials Characterization Laboratory for the AFM work and FE-SEM images (Dr. Jun S. Lee and Dr. Earl Ada) and the assistance of Dr. Sung-Hwan Yoon for providing the etched Si wafers.

REFERENCES

[1] S. Ramakrishna, K. Fujihara, W. Teo, , T. Yong, Z. Ma, and R. Ramaseshan, Materials Today, 3, 40-50, 2006

[2] J. Doshi and D.H. Reneker, Journal of Electrostatics, Vol. 35:151-160, 1995

[3] C.Y. Xu, R. Inai, M. Kotaki, and S. Ramakrishna, Biomaterials, 25, 877-886, 2004

[4] C.Y. Xu, R. Inai, M. Kotaki, and S. Ramkrishana, Tissue Engineering, 10, 1160-1168, 2004

[5] D.S. Katti, K.W. Robinson, F.K. Ko, C.T. Laurencin, Journal of Biomedical Materials Research, Part B: Applied Biomaterials, 286-296, 2004

[6] M. Shin, O. Ishii, T. Sueda, and J.P. Vacanti, Biomaterials, 25, 3717-3723, 2004

[7] H. Yoshimoto, Y.M. Shin, H. Terai, and J.P. Vacanti, Biomaterials, 24, 2077-2082, 2003

[8] C.M. He and M.R. Roach, Journal of Vascular Surgery, 20(1), 6-13, 1994

[9] N.N. Bunyan, J. Chen, I. Chen and S. Farboodmanesh, Polymeric Nanofibers, ed. D.H. Reneker and H. Fong, ACS Symposium Series 918, 106-120, 2006

[10] M.L. Bellan, J. Kameoka, and H.G. Craighead, Nanotechnology, 16, 1095-1099, 2005

[11] E.P.S. Tan and C.T. Lim, Applied Physics Letter, 84(9), 2004